Neuroscience 128 (2004) 209–216

CAPILLARY LEVEL IMAGING OF LOCAL CEREBRAL BLOOD FLOW IN BICUCULLINE-INDUCED EPILEPTIC FOCI

H. HIRASE,* J. CRESO AND G. BUZSÁKI

Center for Molecular and Behavioral Neuroscience Rutgers, The State University of New Jersey, 197 University Avenue, Newark, NJ 07102, USA

Abstract—Local hemodynamics of the cerebral cortex is the basis of modern functional imaging techniques, such as fMRI and PET. Despite the importance of local regulation of the blood flow, capillary level quantification of cerebral blood flow has been limited by the spatial resolution of functional imaging techniques and the depth penetration of conventional optical microscopy. Two-photon laser scanning microscopic imaging technique has the necessary spatial resolution and can image capillaries in the depth of the cortex. We have loaded the serum with fluorescein isothiocyanate dextran and quantified the flow of red blood cells (RBCs) in capillaries in layers 2/3 of the mouse somatosensory cortex *in vivo*. Basal capillary flux was quantified as approximately 28.9±13.6 RBCs/s (n=50, mean±S.D.) under ketamine–xylazine anesthesia and 26.7±16.0 RBCs/s (n=31) under urethane anesthesia. Focal interictal (epileptiform) activity was induced by local infusion of bicuculline methochloride in the cortex. We have observed that capillary blood flow increased as the cortical local field events developed into epileptiform in the vicinity of GABA receptor blockade (<300 μm from the administration site). Local blood flow in the interictal focus increased significantly (42.5±18.5RBCs/s, n=52) relative to the control conditions or to blood flow measured in capillaries at distant (>1 mm from the focus) sites from the epileptic focus (27.8±12.9 RBCs/s, n=30). These results show that hyper-synchronized neural activity is associated with increased capillary perfusion in a localized cortical area. This volume is significantly smaller than the currently available resolution of the fMRI signal.

Key words: cerebral blood flow, interictal spikes, epileptiform events, microcirculation, energy cost.

The possibility that local circulation efficiency can be modulated by the neuronal activity was first raised by Roy and Sherrington (1890). Evidence supporting this suggestion, however, was not available until tools for measuring local cerebral blood flow became available in the 1970s (Olesen, 1971; Kato et al., 1974; Villringer and Dirnagl, 1995, for review). Recently, measurements of surface blood flow by laser-Doppler flowmetry or microscopic fluorescence imaging revealed that the blood flow response occurs within a few seconds following increased neuronal discharge (Lindauer et al., 1993; Malonek et al., 1997; Schulte et al., 2003). Furthermore, recent studies have indicated that synaptic activity of neurons, in addition to production of action potentials, is an important factor for increased blood flow (Mathiesen et al., 2000; Logothetis et al., 2001; Caesar et al., 2003). These results are consistent with the idea that local cerebral blood flow and metabolic demand of neurons (Attwell and Laughlin, 2001) are tightly correlated. Various mechanisms have been proposed for the neural activity-dependent change of the local blood flow including release of nitric oxide (Faraci and Brian Jr., 1994; Iadecola, 1993; Yang et al., 2003) by spiking activity of certain interneurons (Estrada and DeFelipe, 1998), increase of extracellular concentration of potassium ions (Paulson and Newman, 1987; Caesar et al., 1999), or local change of pH by release of lactate from astrocytes (Pellerin and Magistretti, 1994; Magistretti and Pellerin, 1999). Despite these observations, the exact link between neuronal activity and blood flow change has yet to be discovered. An important issue in this regard is the spatial extent of local blood flow regulation in response to changes in neuronal activity.

It has been long recognized that ictal events cause changes in the local blood flow and metabolism. This has been examined in large areas of the brain within the cortex by various techniques including fMRI and PET scans (for review, Duncan et al., 1997) and also at more localized regions by optical imaging of intrinsic signals from the surface of the cortex (Haglund et al., 1992; Schwartz and Bonhoeffer, 2001). Although quantitative investigation of the relationship between blood oxygen level-dependent and neural activity has systematically been addressed in recent studies (Logothetis et al., 2001; Smith et al., 2002), fMRI signal is limited by both spatial and temporal resolution. Meanwhile, surface imaging methods lack depth penetration and quantification of hemodynamics in deeper (>200 μm) layers of the cortex has been difficult.

Direct observation of cortical blood flow using a microscope objective directly mounted on the top of a craniotomy yields a more precise quantification of the circulation (for review, Hudetz, 1997). Monitoring fluorescently labeled serum using the two-photon laser scanning microscope (2-PLSM; Kleinfeld et al., 1998; Brown et al., 2001; Chaigneau et al., 2003) provides both the spatial and temporal resolution to monitor capillary-level circulation as deep as 500 μm from the surface of the brain. We have utilized the 2-PLSM to investigate the spatial extent of

*Correspondence and present address: H. Hirase, RIKEN Brain Science Institute, Neuronal Circuit Mechanisms Research Group, Hirase Research Unit, 2-1, Hirosawa, Wako-shi, Saitama 351-0198, Japan. Tel: +81-48-462-1111x7478; fax: +81-48-467-9652.
E-mail: hirase@brain.riken.jp (H. Hirase).

Abbreviations: CV, coefficient of variation; FITC, fluorescein isothiocyanate fMRI, functional magnetic resonance imaging; IIS, interictal spike; PET, positron emission tomography; RBC, red blood cell; 2-PLSM, two-photon laser scanning microscope.

0306-4522/04$30.00+0.00 © 2004 IBRO. Published by Elsevier Ltd. All rights reserved.
doi:10.1016/j.neuroscience.2004.07.002

capillary-level cerebral hemodynamics of relative to acutely induced epileptic foci.

EXPERIMENTAL PROCEDURES

Subjects and surgery

Male and female C57BL6 mice (20 g–30 g) were used. Animals were deeply anesthetized with either urethane (1.7 g/kg) or ketamine–xylazine cocktail (25 mg ketamine, 6.3 mg xylazine, 0.25 mg acepromazine per 1.0 ml solution, cocktail dosage=3 ml/kg). Two small stainless micro-screws were driven into the bone above the cerebellum. These screws serve as the ground and reference electrodes for the differential recording of local field potential. An insulated metallic head frame (approximately 1 cm×4 cm, thickness 300 μm, with an approximately 3.5 mm diameter hole in the middle) was attached above to the planned craniotomy with cyanoacrylate cement. A craniotomy of diameter approximately 3 mm was performed above the primary somatosensory cortex and the dura was surgically removed. The exposed area was gently superfused with artificial cerebrospinal fluid (in mMol: 125 NaCl, 3 KCl, 10 glucose, 26 $NaHCO_3$, 1.1 NaH_2PO_4, 2 $CaCl_2$, 1 $MgSO_4$; bubbled with 95% O_2 and 5% CO_2). The craniotomy was then covered with 1% agarose (A9793; Sigma, St. Louis, MO, USA) dissolved in phosphate-buffered saline (pH 7.4), and a glass coverslip was placed on the metal frame. This arrangement allowed access for a glass recording electrode from the side as well as minimizing the pulsation of the brain caused by cardiac pressure and breathing.

All procedures were approved by the Rutgers University Animal Institutional Review Board and were in accordance with the National Institutes of Health Guidelines on the Care and Use of Animals in Research. Efforts were made to minimize the number of animals used and their suffering throughout the procedure of the reported experiments.

Electrophysiology

During the recording session, a heating blanket was placed under the animal to maintain body temperature at approximately 37 °C. The electrocardiogram was recorded continuously. Population bursts of cortical neurons (localized "interictal" spikes: IISs) were induced by inserting a large tip (20–50 μm diameter glass pipette, containing 2.5 mM bicuculline methochloride (B110, Sigma) in physiological saline (0.9% w/v NaCl), into the deep layers of the somatosensory cortex. The pipette solution also contained 2–3% fluorescein isothiocyanate (FITC) dextran (10 kDa, FD-10S; Sigma) for visualizing the tip of the pipette. The micropipette also served to record local field potential and multiple unit activity. Large population bursts were reliably induced 20–40 min after the insertion of the pipette.

Imaging

A custom-made 2-PLSM was used as described earlier (Majewska et al., 2000). Briefly, a Ti:S laser (Mira 800F; Coherent Inc., Santa Clara, CA, USA) was pumped by a solid state CW laser (Verdi 8; Coherent) to produce a mode-locked beam (830 nm, approximately 100 fs pulse width at 76 MHz repetition rate). The beam was directed to a modified confocal scanhead (Fluoview 300; Olympus, Japan). The fluorescent signal was first filtered with an emission filter (HQ525, passband 525±25 nm in combination with infra-red blocking BG-39; both from Chroma Technology Corp., Rockingham, VT, USA) and detected by an external photomultiplier tube (R-3896; Hamamatsu Photonics, Japan) with a built-in preamplifier board (F-5 PSU-B; Olympus). Vasculature was visualized by injecting 50–70 μl of physiological saline (0.9% NaCl) with 5% fluorescein isothiocyanate (FITC)-dextran (2MD; FD-2000S; Sigma) in the tail vein.

Data analysis

The data analysis programs were written using Matlab (Mathworks Inc., Natick, MA, USA).

Capillary red blood cell (RBC) flux was quantified from images that were acquired by repeated line scans in the longitudinal direction of a capillary (Fig. 1C, D). The flux was computed by counting the number of dark stripes per unit time. Variance of the line scan data through time was computed for each longitudinal position of the line scan image. This resulted in a function of longitudinal position that had a well-defined peak indicating the position with the highest contrast (Fig. 1E, F). The stripes were detected by setting a threshold to the pixel intensity-time function around the optimal contrast position. The threshold value was determined as $Threshhold=\bar{D}-\alpha\sigma_D$, where $\bar{D}$ and σ_D denote the mean and S.D. of the pixel intensity around the optimal contrast position through time, and α is a factor for the threshold. α is defaulted to 0.4. In some recordings, the value of α was changed manually to correctly perform the RBC detection, after visual inspection of the processed results.

RESULTS

Visualization and measurement of capillary level hemodynamics

Blood flow was imaged and quantified in a total of 163 capillaries from 26 animals. This included eight animals under urethane anesthesia and 18 animals under ketamine–xylazine anesthesia. Among the ketamine–xylazine-anesthetized population, IISs were induced in 12 animals. Microvessels that had the inner diameter (i.e. FITC filled portion) of less than or equal to 6 μm are considered to be capillaries.

Capillary blood flow can be quantified in terms of the flux (number of traveling RBCs per unit time), velocity (distance that a RBC travels per unit time), or linear density (number of RBCs contained per unit length of the capillary; Kleinfeld et al., 1998). Although velocity has the advantage of achieving a finer temporal resolution, the scan direction must be perfectly parallel to the longitudinal axis of the capillary which is not always obtainable as capillary geometry convolutes in complex shape in three dimensions. We have therefore chosen RBC flux to quantify changes in local circulation.

After the electrode for local field potential recording was inserted in the cerebral cortex, the vasculature was visualized immediately following the i.v. injection of FITC dextran via the tail vein (Fig. 1A, C). The focal plane was adjusted to 200 to approximately 300 μm from the pial surface and blood flow of a selected capillary was imaged by taking repeated fast (approximately 600 Hz) line scans over the capillary (Fig. 1D). Quantification of RBC flux was done off line (Fig. 1E, F, and G; see the Experimental Procedures section).

Quantification of flux under basal conditions

Basal capillary flow was calculated in 50 capillaries under ketamine–xylazine anesthesia (Fig. 2). The mean blood flux was 28.93±13.63 RBC/s (mean±S.D., median=26.68 RBC/s) ranging from 8.94 RBC/s to 59.98 RBC/s. Basal capillary flow under urethane-anesthetized animals was quantified in 31 capillaries as 26.86±15.97 RBC/s (medi-

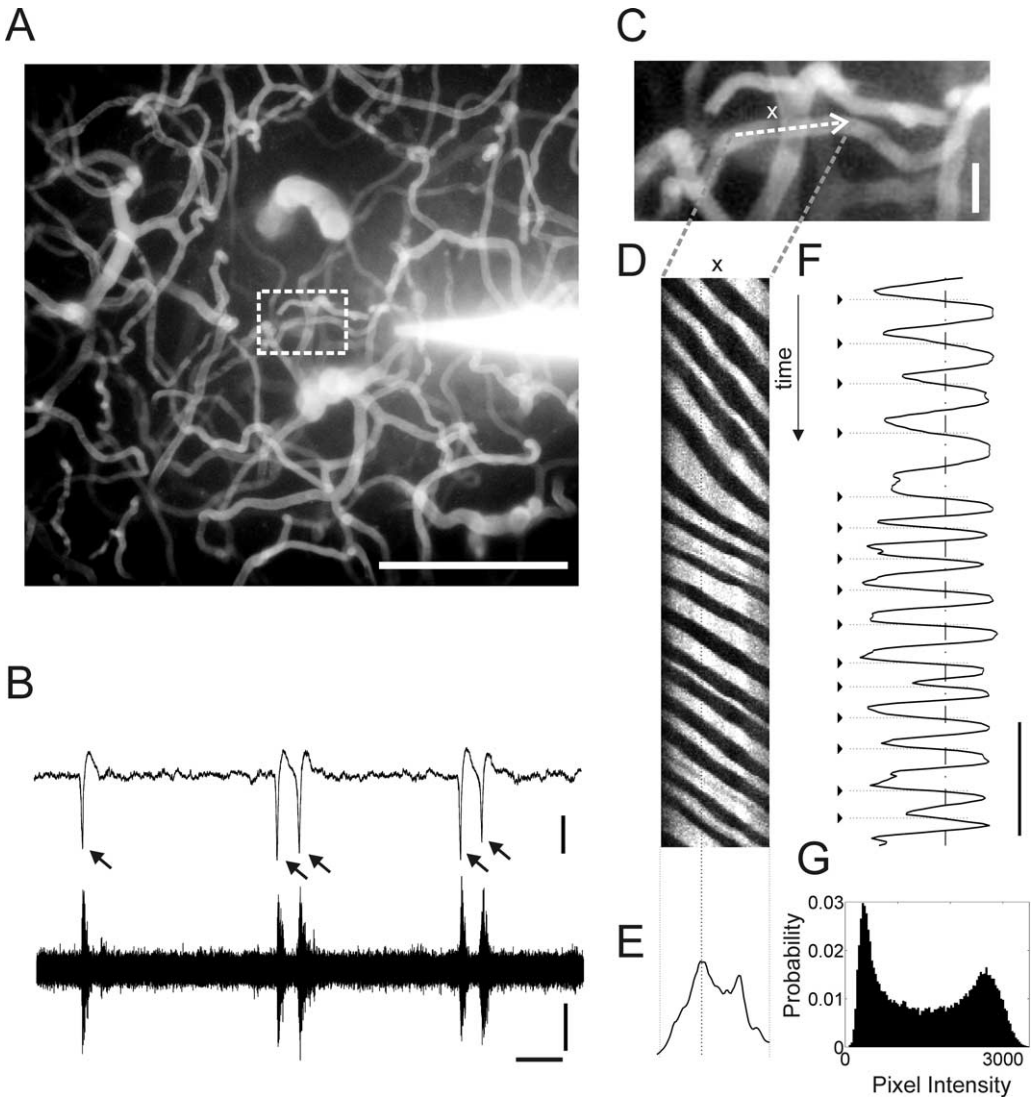

Fig. 1. Imaging and quantification of capillary level local cerebral blood flow. (A) Organization of vasculature is visualized with 2PLSM from depth approximately 100 μm to 400 μm *in vivo*. The tip of a recording/bicuculline infusion electrode is also visualized. Scale bar=100 μm. (B) In a subset of the experiments, bicuculline methochloride (2.5 mM) was contained in the pipette solution, resulting in induction of hyper-synchronized neural activity known as IISs (single arrows). IISs often exceeds 2 mV in amplitude when recorded with wide-band (upper trace, passband: 1 Hz-3kHz, scale bar=1.0 mV) and as characterized by appearance of high frequency activity (300 Hz–3 kHz, passband: 300 Hz–3 kHz, vertical scale bar=50 μV, horizontal scale bar=1 s) reflecting associated multi-unit activity. (C) Part of image (dotted square) was further digitally magnified (scale bar=10 μm) to select a capillary to quantify blood flow dynamics. The selected capillary is repeatedly scanned in a single line at approximately 600 Hz, resulting in an image with slanted stripes (D). Pixel intensity variance of each column of the image was computed (E) and pixel intensity histogram was computed for the vicinity of the column where the variance was largest (single arrow). (G) The pixel intensity histogram is typically bimodal where presence of RBC is characterized by small pixel intensity values and absence of RBC is indicated by large pixel intensity values. An appropriate threshold was determined for the pixel intensity function (see Experimental Procedures) and the timings of RBC passage were detected by identifying the negative crossings at the threshold (F).

an=22.19 RBC/s) ranging from 8.93 RBC/s to 86.41 RBC/s. The mean capillary flux between the two populations did not differ significantly (*t*-test, $P=0.54$).

In order to assess the effect of laser illumination on blood flow, RBC flux was computed in 1.0 s bins and the correlation coefficient was calculated between time and flux for each capillary. The distribution of correlation coefficients was symmetric and centered to zero. The mean value of the correlation coefficients ($\bar{r}=0.10$) was not significantly different from zero (*t*-test, $P=0.077$), indicating that there is little monotonic tendency of increased or decreased blood flow at the population level due to the near infrared mode lock laser irradiation. Similar results were attained with larger (time bin=2.0 s) and smaller (time bin=0.5 s) bins.

Development of interictal event

Under both urethane and ketamine anesthesia, cortical neural activity was characterized by appearance of alter-

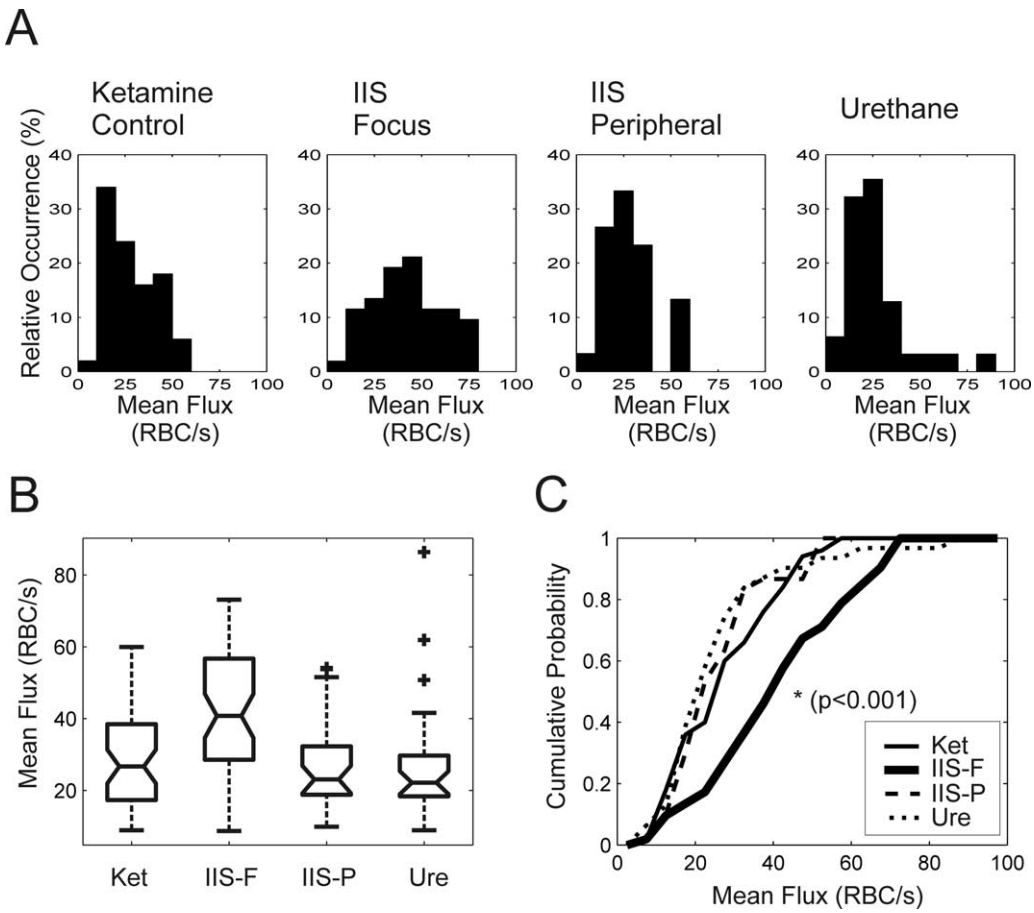

Fig. 2. Distributions of mean capillary blood flow. (A) Histograms of mean capillary RBC flux are plotted for ketamine-anesthetized animals (control), IIS focus (IIS-F; within 300 μm of the bicuculline infusion site), peripheral to IIS focus (IIS-P; farther than 1.0 mm from the bicuculline infusion site), and urethane-anesthetized animals. (B) The summary of the distributions of mean capillary RBC flow in different experiments is presented with box plots. The horizontal line at the notch of each of the boxes represents the median value and the whiskers represent the upper and lower quartiles. Outlier data points are plotted with crosses (+). (C) Cumulative probability was plotted for ketamine-anesthetized animals (control), IIS-F, IIS-P, and urethane-anesthetized animals. Kolmogorov-Smirnov test indicates that IIS-F blood flux is significantly higher ($P<0.001$) than that of the control conditions.

nating synchronized state and quiescence state at 1 to 3 s interval, sometimes referred to as 'up-state' and 'down-state'. The magnitude of synchronized activity ranged from approximately 200 to 400 μV in amplitude. When bicuculline containing recording electrode was inserted, the occurrences of up-states and down-states persisted for the first 10 min. The oscillatory appearance of up-states gradually transformed into larger amplitude oscillation and occasionally elicited sharp negative deflections. The sharp negative deflections developed to large IISs 20 to 40 min after the bicuculline containing recording electrode was inserted. Overall, the inter spike interval of interictal events was 3.69±1.68 s and the mean amplitude was 3.00±0.60 mV (Fig. 1B).

Blood flow during epileptiform conditions

Once epileptiform condition was fully developed, capillary blood flow was measured within 300 μm from the tip of the bicuculline containing electrode (Fig. 1). Mean capillary flux of 52 in-epileptic-focus capillaries were calculated to be 42.51±18.54 RBC/s (median=40.79 RBC/s) ranging from 8.69 RBC/s to 73.17 RBC/s. At the population level, the mean capillary RBC flux in the epileptic foci was approximately 47% higher than the basal condition of ketamine-anesthetized experiments. The increase of capillary flux in epileptic foci compared with that of basal condition was statistically significant (*t*-test, $P<0.00005$). Next, 30 capillaries peripheral to the epileptic focus (>1.0 mm away from the tip of the bicuculline containing electrode, 'off-epileptic-focus') were randomly sampled and flux on each capillary in the presence of IISs was computed. Mean flux of off-epileptic-focus capillaries was computed to be 27.28±12.19 RBC/s (median=23.07 RBC/s, range=[9.90, 54.14] RBC/s). When compared with in-epileptic-focus capillary flow, the mean flux of off-epileptic-focus flux was significantly lower (*t*-test, $P<0.0001$); however, it was not significantly different from that of ketamine-anesthetized control (*t*-test, $P=0.59$).

Heartbeat rates during epileptic conditions were compared with that of pre-epileptic control periods. A pairwise

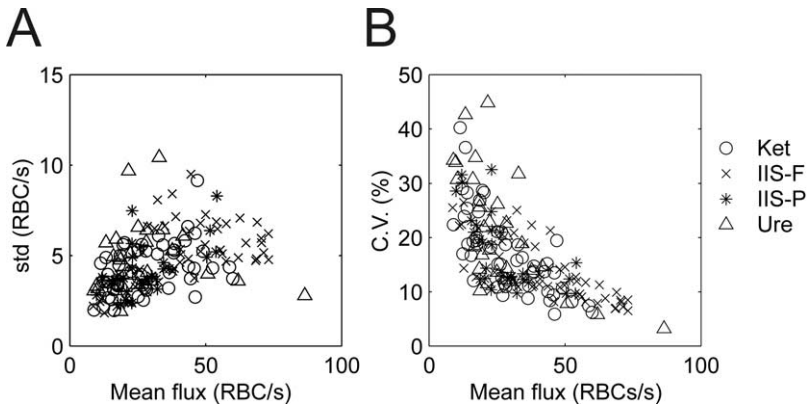

Fig. 3. Time variation of capillary blood flow (bin size=1.0 s). (A) S.D. of RBC flux is plotted against the mean (ordinate) RBC flux for each of the imaged capillaries. (B) CV of RBC flux is plotted against the mean RBC flux for each of the imaged capillaries.

comparison indicated that the heart rate decreased by 0.12 Hz on average in epileptic conditions; however, the difference was not statistically significant (paired *t*-test, $P=-0.11$).

Time variation of RBC flux

We investigated how variable the blood flux was over the imaging period by dividing the RBC flux into 1.0 s bins. S.D. of time binned flux was plotted against mean flux. There is a general positive correlation between the mean flux of a capillary and the S.D. of capillary flux in all experimental conditions (rank correlation $r_o=0.44$ ($P<0.005$), $r_o=0.30$ ($P=0.052$), $r_o=0.55$ ($P<0.0001$), $r_o=0.55$ ($P<0.005$), $r_o=0.54$ ($P<0.0001$), for ketamine–xylazine-anesthetized, urethane-anesthetized, epileptic focus, epileptic peripheral and combined data, respectively; Fig. 3A). Next, coefficient of variation (CV; S.D. normalized to the mean of the distribution) was computed for each capillary. There was an apparent inverse relationship between the mean flux and CV (Fig. 3B). The inverse of CV and the mean flux has a strikingly high degree of linear correlation ($r=0.78$, $P<0.00001$, slope=0.1655 s/RBCs, offset=1.92).

Time dependent changes in blood flux were assessed by computing correlation coefficient between 1.0 s binned blood flux and time for each capillary in epileptic focus. The mean value of the correlation coefficients ($\bar{r}=-0.012$) was not significantly different from zero (*t*-test, $P=0.79$). In addition, the mean value of the correlation coefficients of flux and time for the capillaries located far (>1.0 mm) from the epileptic focus was ($\bar{r}=0.15$) and was not significantly different from zero (*t*-test, $P=0.10$). Similar results were obtained for time bins 0.5 s and 2 s time bins for both the focus and surround capillary data.

In a small subset ($n=6$) of capillaries in the epileptic focus, capillary RBC flux was monitored as the epileptiform condition developed after the insertion of a bicuculline containing recording electrode. RBC flux was monitored by taking 90 s periods of imaging sessions every 5–10 min during the induction of epilepsy. On average, there was 71.9% increase of blood flow after the IISs were induced (paired *t*-test, $P<0.01$). There was a general time-dependent increase of the blood flow within the imaging sessions ($\bar{r}=0.219$, 1.0 s time bin, $P<0.005$). In order to investigate if there is a long term increase of RBC flux due to the induction of epileptiform events, the calculated RBC flux was normalized to the bicuculline infusion time point. When plotted with 10 min interval, there was a high positive correlation between the percentile RBC flux and the bicuculline infusion time (Fig. 4, $r=0.65$, $P<0.0005$).

Distance relationship of RBC flux at epileptic focus

In order to assess the spatial relationship of the capillary blood flow relative to the epileptic focus, we plotted the mean RBC flux against the distance of the capillary to the bicuculline infusion site for each of the proximally located imaged capillaries (Fig. 5). There is a negative correlation between the distance of the imaged capillary to the bicuculline infusion site and the mean RBC flux ($r=-0.289$, $P<0.05$).

DISCUSSION

Two-photon imaging of capillaries filled with fluorescently labeled serum yields the highest time and spatial resolution of blood flow among currently available techniques for blood flow measurements. We have utilized 2-PLSM to investigate capillary level blood flow in layer II/III of the somatosensory cortex in both basal conditions and bicuculline-induced epileptic conditions. As a result, we found a reliable relationship between activity changes of neurons and intracortical blood circulation. Bicuculline was locally infused from the same glass pipette that recorded local field potential. The electrode/infusion site was visualized *in vivo* by labeling the pipette internal solution with a biologically inert fluorescence material. As our approach allowed changing neuronal activity in a circumscribed small volume and precisely identifying the focus of the induced activity, the spatial extent of the increased local blood flow was able to be quantitatively determined.

Our measurement of basal level capillary blood flow (mean=28.93 RBC/s) was compatible with prior measurements using confocal microscope (Dirnagl et al., 1992; Sey-

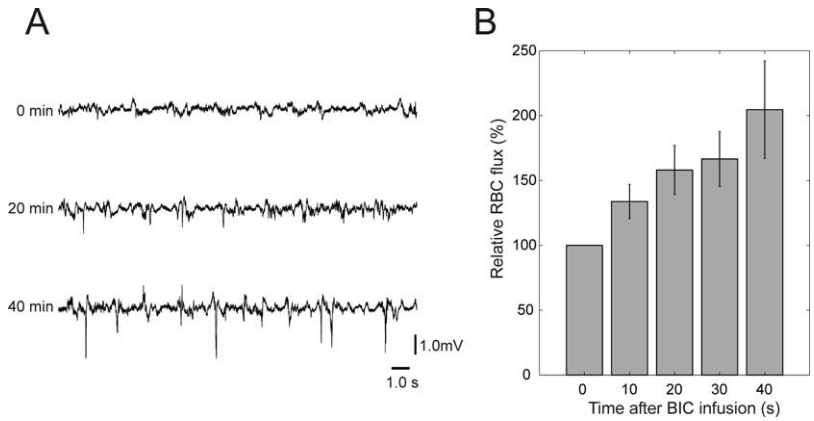

Fig. 4. Time dependence of capillary blood flow in epileptic foci. Capillary RBC was normalized to the point where bicuculline containing electrode was inserted to the imaging area. Relative flux was plotted for the different time points since the infusion of bicuculline. Note that there is a positive correlation between the percentile RBC flux and the bicuculline infusion time ($r=0.65$, $P<0.0005$).

laz et al., 1999) and two-photon microscope (Chaigneau et al., 2003); however, it was slightly lower than the measurements reported by Kleinfeld et al. (1998). While the exact cause of this discrepancy remains to be elucidated, the difference likely may have arisen from the level of anesthesia. In our experiments, the animal was deeply anesthetized with either urethane or ketamine and the mean heart rate during the experiment was approximately 2.5 Hz. It is also conceivable that the species difference contributed to the discrepancy.

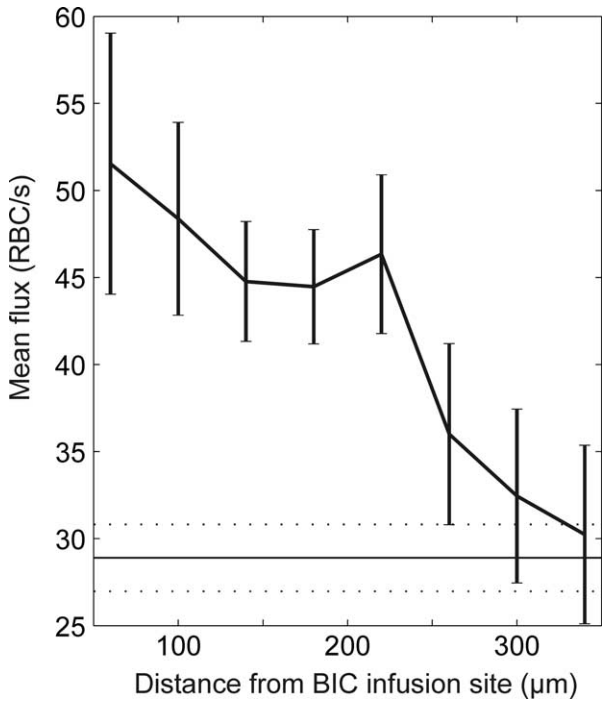

Fig. 5. Distance dependence of capillary blood flow in epileptic foci. Mean RBC flux was plotted against the mean distance of the measured capillaries relative to the bicuculline infusion site. There is a monotonic decrease of capillary RBC flux with the increase of the distance ($r=-0.289$, $P<0.05$). Error bars are expressed in standard error of the mean. The solid and dotted thin horizontal lines indicate the mean flux in the control conditions and the standard error of the mean, respectively.

After bicuculline methochloride was locally infused to the recording site, the field potential elicited IISs that reflected hyper-synchronized neural discharges. Increased synchrony does not necessarily reflect increased neuronal activity; however, previous unit level analysis of epileptiform events indicate that the firing rate of neurons integrated over tens of seconds also increases (Bragin et al., 1997). These synchronized population patterns may remain remarkably localized and involve neuronal populations in a small volume (<300 μm; Bragin et al., 1997). In addition, a recent cortical imaging study using a voltage sensitive dye demonstrates that local application of bicuculline induces IISs in the drug application site (Ma et al., 2004), supporting similar conclusions by previous optical imaging studies of intrinsic signals (Schwartz and Bonhoeffer, 2001). In agreement with this study, we have observed that the peripheral blood flow (>1 mm away from the bicuculline infusion site) did not show any significant difference from the control condition. Furthermore, our results indicate that capillary RBC flux in the epileptic foci is on average approximately 50% higher than that of the basal condition. Also, the rate of heartbeat did not change significantly during the presence of IISs, suggesting that the systemic respiratory pattern or metabolic demand was not affected by the local infusion of bicuculline. Taken together, our results suggest that capillary blood flow increases occurred only in the epileptic foci, where locally increased synchrony in neural activity was induced.

The amount of RBC flux increase in epileptic foci is comparable to the peak transient increase of blood flow triggered by local increase of neural activity induced by sensory stimulus in the cortex (Woolsey et al., 1996; Kleinfeld et al., 1998), olfactory cortex (Chaigneau et al., 2003) or by electrically triggered neural activation (Mathiesen et al., 1998; Schulte et al., 2003). The average amount of blood flow in the bicuculline-induced epileptic foci appears somewhat smaller than the cerebral blood flow increase measured after induction of full seizures reported in previ-

ous studies (Nehlig et al., 1995; Andre et al., 2002). These full seizure models, unlike IISs, have continual discharge of neurons and are less localized in space; therefore, the metabolic demand required by the ictal events is considered to be higher.

There was a statistically significant negative correlation between the mean flux and the distance from the bicuculline infusion site. It is notable that the negative correlation was obtained within the epileptic focus (i.e. approximately <300 μm from the bicuculline infusion site). With the superceding spatial resolution of the multi-photon laser scanning microscope, we have demonstrated that there is a finer gradient in the blood flux within the epileptic focus. Such a gradient could not be obtained by fMRI, as the current spatial resolution of fMRI is approximately 500 μm (Cheng et al., 2001).

Currently, the scan range is limited to one or two capillaries due to the necessity to perform line scans. Simultaneous measurements of a population of capillaries are desired in order to make this mapping technique clinically useful. However, conventional galvanometer-based laser beam scan heads are too slow to achieve the temporal resolution required to achieve flux measurement of capillaries in frame (xy-t) scans. This problem may be circumvented by use of the random access fluorescent microscopy that make use of acoustico-optical deflectors (Bullen et al., 1997), as vasculature occupies less than 10% of the scanned image area. Such a scanner was recently utilized with the multi-photon microscope (Lechleiter et al., 2002). Alternatively, faster scan rates for multi-photon microscopy are available by using a resonant galvanometer mirror (Fan et al., 1999), a rotating polygonal mirror (Bullen et al., 1997), or a microlens array (Bewersdorf et al., 1998).

In conclusion, we have shown that there is a local increase of cerebral of blood flow in the epileptic foci with the 2-PLSM. With the resolution that is an order of magnitude better than other functional imaging techniques, we observed a distance dependent blood flux relationship relative to the epilepsy induction site. Our results and analyses suggest that it is possible to visualize epileptogenic sites with a collection of capillary flux statistics. It is expected that this method can be generalized to detect other metabolically abnormal pathological conditions such as oncogenesis in the brain.

Acknowledgments—We thank A. G. Hudetz, D. L. Buhl, and A. Sirota for their critical comments on an earlier version of this manuscript. This work was supported by National Institutes of Health grant NS043157 (G.B.) and by the Epilepsy Foundation (H.H.).

REFERENCES

Andre V, Henry D, Nehlig A (2002) Dynamic variations of local cerebral blood flow in maximal electroshock seizures in the rat. Epilepsia 43:1120–1128.

Attwell D, Laughlin SB (2001) An energy budget for signaling in the grey matter of the brain. J Cereb Blood Flow Metab 21:1133–1145.

Bewersdorf J, Pick R, Hell SW (1998) Multifocal multiphoton microscopy. Optics Lett 23:655–657.

Bragin A, Csicsvari J, Penttonen M, Buzsaki G (1997) Epileptic after-discharge in the hippocampal-entorhinal system: current source density and unit studies. Neuroscience 76:1187–1203.

Brown EB, Campbell RB, Tsuzuki Y, Xu L, Carmeliet P, Fukumura D, Jain RK (2001) In vivo measurement of gene expression, angiogenesis and physiological function in tumors using multiphoton laser scanning microscopy. Nat Med 7:864–868.

Bullen A, Patel SS, Saggau P (1997) High-speed, random-access fluorescence microscopy: I. High-resolution optical recording with voltage-sensitive dyes and ion indicators. Biophys J 73:477–491.

Caesar K, Akgoren N, Mathiesen C, Lauritzen M (1999) Modification of activity-dependent increases in cerebellar blood flow by extracellular potassium in anaesthetized rats. J Physiol 520(Pt 1): 281–292.

Caesar K, Thomsen K, Lauritzen M (2003) Dissociation of spikes, synaptic activity, and activity-dependent increments in rat cerebellar blood flow by tonic synaptic inhibition. Proc Natl Acad Sci USA 100:16000–16005.

Chaigneau E, Oheim M, Audinat E, Charpak S (2003) Two-photon imaging of capillary blood flow in olfactory bulb glomeruli. Proc Natl Acad Sci USA 100:13081–13086.

Cheng K, Waggoner RA, Tanaka K (2001) Human ocular dominance columns as revealed by high-field functional magnetic resonance imaging. Neuron 32:359–374.

Dirnagl U, Villringer A, Einhaupl KM (1992) In-vivo confocal scanning laser microscopy of the cerebral microcirculation. J Microsc 165(Pt 1):147–157.

Duncan R, Biraben A, Patterson J, Hadley D, Bernard AM, Lecloirec J, Vignal JP, Chauvel P (1997) Ictal single photon emission computed tomography in occipital lobe seizures. Epilepsia 38:839–843.

Estrada C, DeFelipe J (1998) Nitric oxide-producing neurons in the neocortex: morphological and functional relationship with intraparenchymal microvasculature. Cereb Cortex 8:193–203.

Fan GY, Fujisaki H, Miyawaki A, Tsay RK, Tsien RY, Ellisman MH (1999) Video-rate scanning two-photon excitation fluorescence microscopy and ratio imaging with chameleons. Biophys J 76:2412–2420.

Faraci FM, Brian JE Jr (1994) Nitric oxide and the cerebral circulation. Stroke 25:692–703.

Haglund MM, Ojemann GA, Hochman DW (1992) Optical imaging of epileptiform and functional activity in human cerebral cortex. Nature 358:668–671.

Hudetz AG (1997) Blood flow in the cerebral capillary network: a review emphasizing observations with intravital microscopy. Microcirculation 4:233–252.

Iadecola C (1993) Regulation of the cerebral microcirculation during neural activity: is nitric oxide the missing link? Trends Neurosci 16:206–214.

Kato M, Ueno H, Black P (1974) Regional cerebral blood flow of the main visual pathways during photic stimulation of the retina in intact and split-brain monkeys. Exp Neurol 42:65–77.

Kleinfeld D, Mitra PP, Helmchen F, Denk W (1998) Fluctuations and stimulus-induced changes in blood flow observed in individual capillaries in layers 2 through 4 of rat neocortex. Proc Natl Acad Sci USA 95:15741–15746.

Lechleiter JD, Lin DT, Sieneart I (2002) Multi-photon laser scanning microscopy using an acoustic optical deflector. Biophys J 83:2292–2299.

Lindauer U, Villringer A, Dirnagl U (1993) Characterization of CBF response to somatosensory stimulation: model and influence of anesthetics. Am J Physiol 264:H1223–H1228.

Logothetis NK, Pauls J, Augath M, Trinath T, Oeltermann A (2001) Neurophysiological investigation of the basis of the fMRI signal. Nature 412:150–157.

Ma HT, Wu CH, Wu JY (2004) Initiation of spontaneous epileptiform events in the rat neocortex in vivo. J Neurophysiol 91:934–945.

Magistretti PJ, Pellerin L (1999) Cellular mechanisms of brain energy metabolism and their relevance to functional brain imaging. Philos Trans R Soc Lond B Biol Sci 354:1155–1163.

Majewska A, Brown E, Ross J, Yuste R (2000) Mechanisms of calcium decay kinetics in hippocampal spines: role of spine calcium pumps and calcium diffusion through the spine neck in biochemical compartmentalization. J Neurosci 20:1722–1734.

Malonek D, Dirnagl U, Lindauer U, Yamada K, Kanno I, Grinvald A (1997) Vascular imprints of neuronal activity: relationships between the dynamics of cortical blood flow, oxygenation, and volume changes following sensory stimulation. Proc Natl Acad Sci USA 94:14826–14831.

Mathiesen C, Caesar K, Akgoren N, Lauritzen M (1998) Modification of activity-dependent increases of cerebral blood flow by excitatory synaptic activity and spikes in rat cerebellar cortex. J Physiol 512 (Pt 2):555–566.

Mathiesen C, Caesar K, Lauritzen M (2000) Temporal coupling between neuronal activity and blood flow in rat cerebellar cortex as indicated by field potential analysis. J Physiol 523(Pt 1):235–246.

Nehlig A, Vergnes M, Hirsch E, Boyet S, Koziel V, Marescaux C (1995) Mapping of cerebral blood flow changes during audiogenic seizures in Wistar rats: effect of kindling. J Cereb Blood Flow Metab 15:259–269.

Olesen J (1971) Contralateral focal increase of cerebral blood flow in man during arm work. Brain 94:635–646.

Paulson OB, Newman EA (1987) Does the release of potassium from astrocyte endfeet regulate cerebral blood flow? Science 237:896–898.

Pellerin L, Magistretti PJ (1994) Glutamate uptake into astrocytes stimulates aerobic glycolysis: a mechanism coupling neuronal activity to glucose utilization. Proc Natl Acad Sci USA 91:10625–10629.

Roy CS, Sherrington CS (1890) On the regulation of the blood supply of the brain. J Physiol 11:85–108.

Schulte ML, Wood JD, Hudetz AG (2003) Cortical electrical stimulation alters erythrocyte perfusion pattern in the cerebral capillary network of the rat. Brain Res 963:81–92.

Schwartz TH, Bonhoeffer T (2001) In vivo optical mapping of epileptic foci and surround inhibition in ferret cerebral cortex. Nat Med 7:1063–1067.

Seylaz J, Charbonne R, Nanri K, Von Euw D, Borredon J, Kacem K, Meric P, Pinard E (1999) Dynamic in vivo measurement of erythrocyte velocity and flow in capillaries and of microvessel diameter in the rat brain by confocal laser microscopy. J Cereb Blood Flow Metab 19:863–870.

Smith AJ, Blumenfeld H, Behar KL, Rothman DL, Shulman RG, Hyder F (2002) Cerebral energetics and spiking frequency: the neurophysiological basis of fMRI. Proc Natl Acad Sci USA 99:10765–10770.

Villringer A, Dirnagl U (1995) Coupling of brain activity and cerebral blood flow: basis of functional neuroimaging. Cerebrovasc Brain Metab Rev 7:240–276.

Woolsey TA, Rovainen CM, Cox SB, Henegar MH, Liang GE, Liu D, Moskalenko YE, Sui J, Wei L (1996) Neuronal units linked to microvascular modules in cerebral cortex: response elements for imaging the brain. Cereb Cortex 6:647–660.

Yang G, Zhang Y, Ross ME, Iadecola C (2003) Attenuation of activity-induced increases in cerebellar blood flow in mice lacking neuronal nitric oxide synthase. Am J Physiol Heart Circ Physiol 285:H298–H304.

(Accepted 6 July 2004)